



Investigations of Molecular Interactions in the Binary Mixtures of 1-Butyl-3-methylimidazolium bis(Trifluoromethanesulfonyl) Amide and 2-Propoxyethanol from $T = (298.15 \text{ to } 323.15) \text{ K}$ at Atmospheric Pressure

G. Prasad^{1,5} · K. Muralidhar Reddy² · R. Padamasuvarna¹ · T. Madhu Mohan³ · T. Vijaya Krishna³ · S. Govardhana Rao⁴

Received: 5 March 2018 / Accepted: 16 September 2018 / Published online: 19 November 2018
© Springer Science+Business Media, LLC, part of Springer Nature 2018

Abstract

Density and speed of sound values of pure and binary mixtures of 1-butyl-3-methylimidazolium bis(trifluoromethanesulfonyl) amide ([Bmim][NTf₂]) and 2-propoxyethanol (2-PR) were determined over the whole composition range as a function of temperature from 298.15 to 323.15 K) under atmospheric pressure. Heat capacity values of the pure compounds were also measured. The experimental values were used to calculate excess molar volume, excess isentropic compressibility, excess intermolecular free length and excess speed of sound values. The excess values were fitted with the Redlich–Kister polynomial equation to estimate the binary coefficients and standard deviation between the experimental and calculated values. The partial molar volumes at infinite dilutions were also calculated. The trends of variation of these properties were interpreted in light of the solute–solvent interactions occurring in the system. Further, the molecular interactions in the binary system were analyzed using experimental FT-IR spectra recorded at room temperature.

Keywords 1-Butyl-3-methylimidazolium bis(trifluoromethanesulfonyl) amide · 2-Propoxyethanol · Excess molar volume · Infinite dilution · FT-IR

1 Introduction

Ionic liquids gained popularity as “environmentally friendly solvents” and alternatives to “volatile organic solvents” [1–4]. In continuation of our previous work on ILs and their binary mixtures with industrially important organic solvents [5–8], in the

Electronic supplementary material The online version of this article (<https://doi.org/10.1007/s10953-018-0833-x>) contains supplementary material, which is available to authorized users.

✉ T. Madhu Mohan
tmadhumohan@gmail.com

✉ T. Vijaya Krishna
tvjayakrishna1980@gmail.com

Extended author information available on the last page of the article

present study we have chosen the binary mixtures of the IL, 1-butyl-3-methylimidazolium bis(trifluoromethanesulfonyl) amide ([Bmim][NTf₂]) and 2-propoxyethanol (2-PR). The relatively low viscosity of imidazolium based ILs facilitates easy handling, adequate performance in extractive applications and thus these ILs are more environmentally friendly than the other ILs [9]. [Bmim][NTf₂] is a preferred ionic liquid as electrolyte for capacitive energy storage and also in the process of nuclear fuel recycling [10]. On the other hand, alkoxyethanols are amphiphilic organic solvents which can be used in many chemical processes. The mixtures containing alkoxyethanols are very important in view of their strong intermolecular effects produced by the presence of –O– and –OH groups in the same compound. 2-PR is used as a solvent in varnishes, dyes and pesticides.

It is well-known that the reaction medium plays an important role in determining reactivity, that is reflected in thermodynamic, transport and spectral properties. The thermodynamic properties of solutions are very useful to obtain information on the intermolecular interactions and geometrical effects in the systems. Moreover, knowledge of the thermodynamic properties of binary mixtures is essential for the proper design of industrial processes. Thus the accurate knowledge of thermodynamic properties of the [Bmim][NTf₂] + 2-PR binary mixture can be of great importance for their possible use in bioreactor technology, Li-ion batteries, synthesis of nano objects, separation technology, catalysis, etc. [11].

2 Experimental Section

2.1 Chemicals Used

The ionic liquid, 1-butyl-3-methylimidazolium bis(trifluoromethanesulfonyl) amide was procured from Io-Li-Tec, Germany and 2-propoxyethanol was procured from Sigma Aldrich, USA. 2-PR was purified by distillation and [Bmim][NTf₂] was used without any further purification.

2.1.1 Analysis of the Water Contents of the Chemicals

The values of water content in [Bmim][NTf₂] and 2-PR were determined using a Karl-Fischer titrator (Metrohm, 890 Titrando). This can detect water content from less than 10 ppm to 100%. All samples were dried for at least 72 h under atmospheric pressure and moderate temperature (beginning at room temperature and increasing gradually up to 333 K over a period of 6 h), before making the measurements. The provenance, CAS number, mass fraction purity and water content values of the pure compounds are given in Table 1.

2.2 Apparatus and Procedure

2.2.1 Sample Preparation

All samples were prepared by mass and were stored in amber colored glass vials (8 mL) with screw caps having PFE septa, sealed with parafilm to prevent absorption of moisture from the atmosphere. The samples were prepared immediately prior to measurement, using an electronic balance (CPA-225D, Sartorius, Germany) with a readability of $\pm 1 \times 10^{-7}$ kg. The uncertainty in the mole fraction was estimated to be within $\pm 1 \times 10^{-4}$.

Table 1 List of chemicals with details of provenance, CAS number, mass fraction purity and water content

Chemical	Provenance	CAS number	Initial mass fraction purity (by supplier)	Purification method	Final mass fraction purity	Water content (ppm)	Analysis method
1-butyl-3-methylimidazolium bis(trifluoromethanesulfonyl) amide	Io-Li-Tec, Germany	174899-83-3	0.995	Used as received	0.995	40	Karl–Fischer titration
2-propoxyethanol	Sigma Aldrich, USA	2807-30-9	0.994	Distillation	0.999	60	Gas liquid chromatography

2.2.2 Measurement of Density and Speed of Sound

The density and speed of sound values of the pure compounds and their binary mixtures were measured using a digital Density and Sound Analyzer (DSA 5000 M, Anton Parr, Austria), which employs the well-known oscillating U-tube principle (for density measurement) and propagation time technique (for speed of sound measurement at a frequency of 3 MHz). The reproducibility of values of density and speed of sound were $\pm 1 \times 10^{-3} \text{ kg}\cdot\text{m}^{-3}$ and $\pm 1 \times 10^{-2} \text{ m}\cdot\text{s}^{-1}$, respectively. The density meter was calibrated with double distilled degassed water ($\rho = 997.075 \text{ kg}\cdot\text{m}^{-3}$ at 298.15 K). After each measurement distilled water and anhydrous ethanol were used to clean the vibrating tube. The reported values are the average of three consecutive measurements carried out between the temperatures (298.15–323.15) K with intervals of 5 K, under atmospheric pressure. The standard uncertainty associated with the measurement of temperature is ± 0.01 K. The estimated uncertainties of density and speed of sound are within $\pm 0.05 \text{ kg}\cdot\text{m}^{-3}$ and $\pm 0.5 \text{ m}\cdot\text{s}^{-1}$, respectively. The comparison of density and speed of sound values with the NIST ThermoLit data at temperatures $T = (298.15\text{--}323.15)$ K is shown in Table 2 [12–21].

2.2.3 Measurement of Heat Capacity and Infrared Spectra

The heat capacity (C_p) values of pure [Bmim][NTf₂] and pure 2-PR were determined with a micro DSC 7 evo (SETARAM instrumentation, France) differential scanning calorimeter. It has a double stage temperature controller which works in the temperature range (228.15–393.15) K, with a heating rate of (0.001–2) K·min⁻¹. A “mixing batch cell” made up of Hastelloy C276 was used with a sample capacity of (10–50) μL . The instrument was calibrated by determining the enthalpy of fusion of naphthalene (147.78 J·g⁻¹) using the Joule effect method. The estimated uncertainty of heat capacity is $u(C_p) = (0.003 \cdot C_p)$ J·K⁻¹·mol⁻¹. The infrared transmittance was measured by using a Shimadzu Fourier transform infrared (FT-IR) spectrometer equipped with attenuated total reflectance (ATR) accessories. The spectral region was 500–3500 cm⁻¹ with resolution of 2 cm⁻¹ and 100 scans. At least five repeated measurements were performed for each sample.

3 Results and Discussion

The density values obtained from the experiments were fitted well with the linear equation,

$$\rho = a + bT \quad (1)$$

where a and b represent the empirical parameters obtained by the method of least squares fitting. The fitting parameters and the average absolute relative deviation (ARD) defined by the Eq. 2 are presented in supplemental Table S1.

$$ARD = \left(\frac{1}{n} \sum \frac{|\rho_{\text{exp}} - \rho|}{\rho_{\text{exp}}} \right) 100 \quad (2)$$

where n is the number of data points, ρ_{exp} is the experimental density and ρ is the calculated density.

The variation of density (ρ) values, as a function of [Bmim][NTf₂] concentration (x_1) and temperature, is shown in Fig. 1. At all investigated temperatures, the density values

Table 2 Comparison of density (ρ) and speed of sound (u) of pure compounds with literature at temperatures from $T = (298.15$ to $323.15)$ K at pressure $p = 0.1$ MPa

Compound	T (K)	ρ ($\text{kg}\cdot\text{m}^{-3}$)		u ($\text{m}\cdot\text{s}^{-1}$)		C_p ($\text{J}\cdot\text{K}^{-1}\cdot\text{mol}^{-1}$)	
		Experimental	Literature	Experimental	Literature	Experimental	Literature
1-butyl-3-methylimidazolium bis(trifluoromethanesulfonyl) amide	298.15	1437.12	1436.8 [12] 1436.50 [13] 1437.7 [14]	1227.8	1226.7 [11] 1227.52 [15]	567.22	567.33 [17]
		1432.51	1432 [12] 1431.69 [13] 1432.9 [14]	1216.7	1215.6 [11] 1217.51 [16]	569.85	569.74 [17]
	308.15	1427.43	1427.2 [12] 1426.90 [13] 1428.0 [14]	1205.8	1204.6 [11]	572.64	572.82 [17]
		1422.86	1422.5 [12] 1422.15 [13] 1423.2 [14]	1194.9	1193.7 [11] 1194.50 [16]	575.47	575.56 [17]
	318.15	1417.91	1417.8 [12] 1417.41 [13] 1418.5 [14]	1184.2	1183.99 [15]	578.38	578.49 [17]
		1413.58	1413.1 [12] 1412.70 [13] 1413.7 [14]	1173.6	1172.58 [16]	581.52	581.68 [17]

Table 2 (continued)

Compound	T (K)		ρ (kg·m ⁻³)		u (m·s ⁻¹)		C_p (J·K ⁻¹ ·mol ⁻¹)	
	Experimental	Literature	Experimental	Literature	Experimental	Literature	Experimental	Literature
2-propoxyethanol	298.15	907.161 [18] 908.0 [19] 908.19 [20] 908.31 [21]	907.21		1300.4	1299.9 [21] 1300.92 [18]	240.96	241.78 [18]
	303.15	902.744 [18] 903.11 [20]	902.83		1282.9	1283.65 [18]	243.02	243.85 [18]
	308.15	898.324 [18]	898.46	899.50 [21]	1265.6	1265.0 [21] 1266.41 [18]	245.09	245.91 [18]
	313.15	893.894 [18]	894.09		1248.4	1249.17 [18]	247.21	247.98 [18]
	318.15	889.454 [18]	889.72	890.56 [21]	1230.6	1230.1 [21] 1231.93 [18]	249.23	250.05 [18]
	323.15	885.004 [18]	885.35		1214.2	1214.95 [18]	251.87	252.11 [18]

Standard uncertainties u are $u(T) = \pm 0.01$ K, $u(\rho) = \pm 0.05$ kg·m⁻³, $u(u) = \pm 0.5$ m·s⁻¹, $u(C_p) = (0.003 \cdot C_p)$ J·K⁻¹·mol⁻¹, $u(p) = \pm 0.002$ MPa

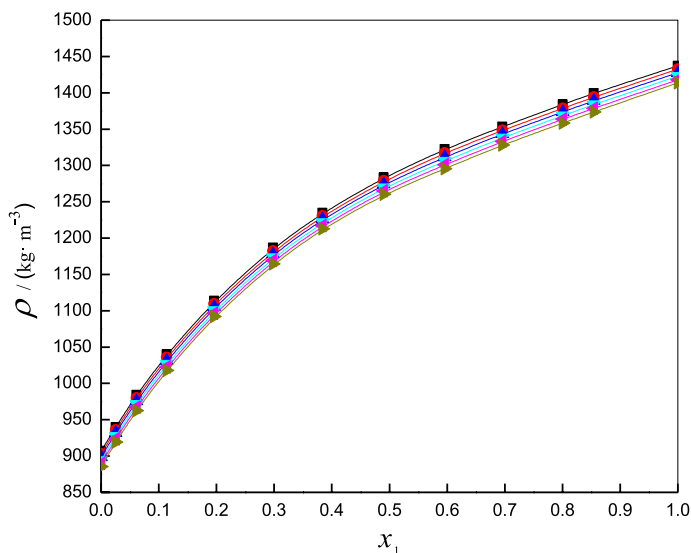


Fig. 1 Density ρ versus mole fraction of [Bmim][NTf₂] (x_1) in the binary mixture of [Bmim][NTf₂] + 2-PR. 298.15 K (filled square), 303.15 K (red filled circle), 308.15 K (blue filled triangle), 313.15 K (green filled inverted triangle), 318.15 K (pink filled left sided triangle) and 323.15 K (light green filled right sided triangle) (Color figure online)

increase with increasing mole fraction of [Bmim][NTf₂] in the mixture and decrease with increasing temperature. The variation of the speed of sound values (u), as a function of [Bmim][NTf₂] concentration and temperature, is shown in Fig. 2. The speeds of sound decrease with increasing mole fraction of [Bmim][NTf₂] and as the temperature increases. The variations in the values of density and speed of sound with respect to mole fraction and temperature (Table 3) demonstrate that the physical properties of [Bmim][NTf₂] can be modified in a controlled way by adding 2-PR or changing the temperature.

V_m values (Table 4) of [Bmim][NTf₂] + 2-PR increase with [Bmim][NTf₂] concentration and with temperature. The increase in the molar volume of a system upon mixing of the components could be attributed to the dissociation of one component or both the components and formation of solute–solvent bonds.

The excess molar volume (V_m^E) was calculated from the equation,

$$V_m^E = \left(\frac{x_1 M_1 + x_2 M_2}{\rho} \right) - \left(\frac{x_1 M_1}{\rho_1} + \frac{x_2 M_2}{\rho_2} \right) \quad (3)$$

where x_1 , x_2 , M_1 , M_2 , ρ_1 and ρ_2 represent the mole fraction, molar mass and density of pure component 1 ([Bmim][NTf₂]) and pure component 2 (2-PR), respectively, and ρ is the density of the binary mixture.

Figure 3 indicates that the V_m^E values exhibit a sigmoid variation, with negative values at low mole fractions of [Bmim][NTf₂] and positive values at high mole fractions of [Bmim][NTf₂] in the binary mixture, over the investigated temperature range. The sign and magnitude of the volume changes that take place on mixing [Bmim][NTf₂] and 2-PR are the result of several effects that operate in the same or in the opposite direction. In general, the physical contributions comprised of dispersion forces and non-specific physical (weak) interactions lead to positive V_m^E values. The chemical contributions, like breaking up of the

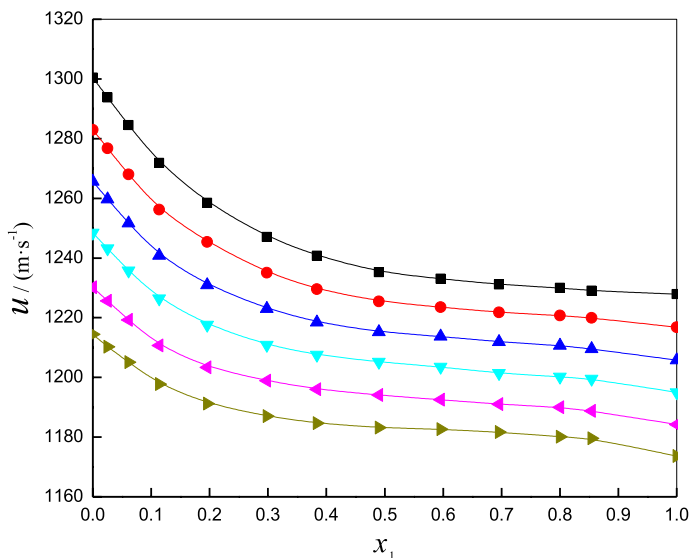


Fig. 2 Speed of sound u versus mole fraction of [Bmim][NTf₂] (x_1) in the binary mixture of [Bmim][NTf₂]+2-PR. 298.15 K (filled square), 303.15 K (red filled circle), 308.15 K (blue filled triangle), 313.15 K (green filled inverted triangle), 318.15 K (pink filled left sided triangle) and 323.15 K (light green filled right sided triangle) (Color figure online)

associates present in the pure liquids, result in positive V_m^E values. Whereas, the chemical contributions such as formation of H-bonding, charge transfer (donor–acceptor) complexes, strong dipole–dipole and ion–dipole interactions between the component species of the mixture result in negative V_m^E values [22].

A plausible qualitative interpretation of the variation of V_m^E with composition has been suggested. On mixing [Bmim][NTf₂] and 2-PR, the disruption of the associations present in pure liquids takes place with subsequent formation of new interactions between unlike species. The negative V_m^E values at low mole fractions of ionic liquid ($x_1 < 0.4901$) suggest the formation of significant ion–dipole interactions between the ions [Bmim]⁺ and [NTf₂][−] formed by the ionic liquid and dipoles of 2-PR species. At higher mole fractions ($x_1 > 0.4901$) the interactions between like species IL–IL and 2-PR–2-PR seem to dominate in the binary mixture.

Comparison of the present system with the literature can provide a clear picture about the nature of molecular interactions. In the 2-PR rich region, the present system ([Bmim][NTf₂]+2-PR) was compared with the [Bmim][PF₆]+2-PR [18] and [Emim][EtSO₄]+2-PR [21] systems. The V_m^E values of [Bmim][PF₆]+2-PR and [Emim][EtSO₄]+2-PR are negative over the complete composition range, at all temperatures. While, the [Bmim][NTf₂]+2-PR system shows a sigmoid variation. Further, more negative values of V_m^E are observed in the case of [Bmim][NTf₂]+2-PR compared with the remaining systems, indicating strong molecular interactions between the species. In the [Bmim][NTf₂] rich region, the present system ([Bmim][NTf₂]+2-PR) was compared with [Bmim][NTf₂]+2-methoxyethanol [23] and [Bmim][NTf₂]+2-ethoxyethanol [24] systems. The V_m^E values of [Bmim][NTf₂]+2-methoxyethanol are negative over the whole composition range at all temperatures. While, [Bmim][NTf₂]+2-ethoxyethanol and [Bmim][NTf₂]+2-PR systems show a sigmoid variation. Further, more positive values of V_m^E are observed in the case of [Bmim][NTf₂]+2-PR compared with [Bmim][NTf₂]+2-ethoxyethanol system, indicating less packing.

Table 3 Density (ρ) and speed of sound (u) with mole fraction (x_1) of 1-butyl-3-methylimidazolium bis(trifluoromethanesulfonyl) amide in the binary mixture of 1-butyl-3-methylimidazolium bis(trifluoromethanesulfonyl) amide + 2-propoxyethanol from $T=(293.15$ to $323.15)$ K at pressure $p=0.1$ MPa

x_1	ρ (kg·m ⁻³)	u (m·s ⁻¹)
$T=298.15$ K		
0	907.21	1300.4
0.0251	939.99	1293.7
0.0614	984.36	1284.5
0.1131	1040.02	1271.9
0.1957	1113.81	1258.5
0.2980	1186.72	1247.0
0.3837	1234.84	1240.8
0.4901	1283.56	1235.3
0.5958	1322.35	1233.1
0.6956	1353.49	1231.1
0.8003	1383.84	1229.9
0.8543	1399.39	1229.1
1	1437.12	1227.9
$T=303.15$ K		
0	902.83	1282.9
0.0251	936.07	1276.7
0.0614	980.06	1268.0
0.1131	1035.62	1256.2
0.1957	1109.45	1245.4
0.2980	1182.29	1235.1
0.3837	1230.42	1229.5
0.4901	1278.94	1225.4
0.5958	1317.06	1223.5
0.6956	1348.41	1221.7
0.8003	1378.76	1220.7
0.8543	1394.23	1219.9
1	1432.51	1216.8
$T=308.15$ K		
0	898.46	1265.6
0.0251	931.85	1259.7
0.0614	975.71	1251.6
0.1131	1031.23	1240.8
0.1957	1105.09	1230.9
0.2980	1177.86	1222.9
0.3837	1226.23	1218.5
0.4901	1274.32	1215.3
0.5958	1311.66	1213.7
0.6956	1343.31	1211.9
0.8003	1373.68	1210.7
0.8543	1389.07	1209.6
1	1427.43	1205.8
$T=313.15$ K		
0	894.09	1248.4
0.0251	927.56	1243.2
0.0614	971.39	1235.7

Table 3 (continued)

x_1	ρ (kg·m ⁻³)	u (m·s ⁻¹)
0.1131	1026.85	1226.4
0.1957	1100.74	1217.6
0.2980	1173.43	1210.9
0.3837	1221.58	1207.5
0.4901	1269.71	1205.1
0.5958	1306.32	1203.5
0.6956	1338.21	1201.5
0.8003	1368.59	1200.2
0.8543	1383.92	1199.5
1	1422.86	1194.9
$T=318.15$ K		
0	889.72	1230.2
0.0251	923.48	1225.6
0.0614	966.98	1219.2
0.1131	1022.46	1210.7
0.1957	1096.39	1203.3
0.2980	1169.03	1198.9
0.3837	1217.16	1196.1
0.4901	1265.09	1194.1
0.5958	1300.98	1192.5
0.6956	1333.12	1191.1
0.8003	1363.51	1189.9
0.8543	1378.76	1188.7
1	1417.91	1184.2
$T=323.15$ K		
0	885.35	1214.4
0.0251	919.22	1210.2
0.0614	962.69	1205.0
0.1131	1018.08	1197.7
0.1957	1092.04	1191.2
0.2980	1164.57	1186.9
0.3837	1212.74	1184.6
0.4901	1260.47	1183.2
0.5958	1295.63	1182.7
0.6956	1328.02	1181.7
0.8003	1358.43	1180.1
0.8543	1373.61	1179.6
1	1413.58	1173.6

Standard uncertainties u are $u(T)=\pm 0.01$ K, $u(x_1)=\pm 1\times 10^{-4}$, $u(\rho)=\pm 0.05$ kg·m⁻³, $u(u)=\pm 0.5$ m·s⁻¹, $u(p)=\pm 0.002$ MPa

Figure 3 shows that V_m^E values become more negative as the temperature is increased in the 2-PR rich region. With increase in temperature the kinetic energy of the species increases, making more and more 2-PR free species available in the mixture due to the breaking of hydrogen bonds. These free alkanol species interact with the ions present in

Table 4 Molar volume (V_m), isentropic compressibility (κ_s), molar isentropic compressibility ($\kappa_{s,m}$) and intermolecular free length (L_f) with mole fraction (x_1) of 1-butyl-3-methylimidazolium bis(trifluoromethanesulfonyl) amide in the binary mixture of 1-butyl-3-methylimidazolium bis(trifluoromethanesulfonyl) amide + 2-propoxyethanol from $T=(298.15$ to $323.15)$ K at pressure $p=0.1$ MPa

x_1	$V_m \times 10^6$ ($\text{m}^3 \cdot \text{mol}^{-1}$)	$\kappa_s \times 10^{12}$ (Pa^{-1})	$\kappa_{s,m} \times 10^{15}$ ($\text{m}^3 \cdot \text{Pa}^{-1} \cdot \text{mol}^{-1}$)	$L_f \times 10^{11}$ (m)
$T=298.15$ K				
0	114.80	651.82	74.83	5.25
0.0251	119.22	635.56	75.77	5.19
0.0614	125.47	615.71	77.25	5.10
0.1131	134.42	594.37	79.90	5.01
0.1957	148.89	566.86	84.40	4.90
0.2980	166.92	541.88	90.45	4.79
0.3837	182.29	526.03	95.89	4.72
0.4901	201.50	510.58	102.88	4.65
0.5958	220.79	497.35	109.81	4.59
0.6956	238.95	487.45	116.48	4.54
0.8003	257.56	477.67	123.03	4.50
0.8543	266.86	473.07	126.24	4.47
1	291.81	461.54	134.68	4.42
$T=303.15$ K				
0	115.36	672.97	77.63	5.38
0.0251	119.72	655.37	78.46	5.31
0.0614	126.02	634.58	79.97	5.23
0.1131	134.99	611.89	82.60	5.13
0.1957	149.48	581.17	86.87	5.00
0.2980	167.54	554.52	92.91	4.89
0.3837	182.95	537.57	98.35	4.81
0.4901	202.23	520.64	105.29	4.74
0.5958	221.67	507.19	112.43	4.67
0.6956	239.85	496.82	119.16	4.63
0.8003	258.51	486.70	125.82	4.58
0.8543	267.85	481.95	129.09	4.56
1	292.75	471.50	138.03	4.51
$T=308.15$ K				
0	115.92	694.82	80.54	5.52
0.0251	120.26	676.27	81.33	5.45
0.0614	126.58	654.19	82.81	5.36
0.1131	135.57	629.86	85.39	5.26
0.1957	150.07	597.16	89.62	5.12
0.2980	168.17	567.64	95.46	4.99
0.3837	183.57	549.27	100.83	4.91
0.4901	202.96	531.34	107.84	4.83
0.5958	222.59	517.53	115.20	4.76
0.6956	240.76	506.89	122.04	4.72
0.8003	259.46	496.66	128.86	4.67
0.8543	268.84	492.06	132.29	4.65

Table 4 (continued)

x_1	$V_m \times 10^6$ ($\text{m}^3 \cdot \text{mol}^{-1}$)	$\kappa_s \times 10^{12}$ (Pa^{-1})	$\kappa_{s,m} \times 10^{15}$ ($\text{m}^3 \cdot \text{Pa}^{-1} \cdot \text{mol}^{-1}$)	$L_f \times 10^{11}$ (m)
1	293.79	481.83	141.56	4.60
$T(\text{K}) = 313.15$				
0	116.49	717.64	83.60	5.66
0.0251	120.81	697.52	84.27	5.58
0.0614	127.14	674.12	85.71	5.49
0.1131	136.15	647.49	88.15	5.38
0.1957	150.66	612.80	92.33	5.23
0.2980	168.81	581.24	98.12	5.09
0.3837	184.27	561.43	103.45	5.01
0.4901	203.70	542.28	110.46	4.92
0.5958	223.50	528.50	118.12	4.86
0.6956	241.68	517.68	125.11	4.81
0.8003	260.43	507.26	132.10	4.76
0.8543	269.84	502.20	135.51	4.74
1	294.74	492.20	145.07	4.69
$T(\text{K}) = 318.15$				
0	117.06	742.71	86.94	5.81
0.0251	121.35	720.88	87.48	5.72
0.0614	127.72	695.61	88.85	5.62
0.1131	136.73	667.23	91.23	5.51
0.1957	151.29	629.91	95.30	5.35
0.2980	169.44	595.17	100.85	5.20
0.3837	184.94	574.35	106.22	5.11
0.4901	204.44	554.37	113.34	5.02
0.5958	224.41	540.52	121.30	4.96
0.6956	242.60	528.80	128.29	4.90
0.8003	261.40	517.91	135.38	4.85
0.8543	270.85	513.27	139.02	4.83
1	295.77	502.90	148.74	4.78
$T(\text{K}) = 323.15$				
0	117.64	765.84	90.09	5.95
0.0251	121.91	742.69	90.54	5.86
0.0614	128.29	715.28	91.76	5.75
0.1131	137.32	684.72	94.03	5.63
0.1957	151.89	645.36	98.02	5.46
0.2980	170.09	609.47	103.67	5.31
0.3837	185.61	587.57	109.06	5.21
0.4901	205.19	566.74	116.29	5.12
0.5958	225.34	551.81	124.35	5.05
0.6956	243.53	539.25	131.32	4.99
0.8003	262.38	528.59	138.69	4.94
0.8543	271.87	523.24	142.25	4.92
1	296.67	513.61	152.37	4.87

Standard uncertainties u are $u(T) = \pm 0.01$ K, $u(x_1) = \pm 1 \times 10^{-4}$, $u(V_m) = \pm 0.05 \times 10^{-6}$ $\text{m}^3 \cdot \text{mol}^{-1}$, $u(\kappa_s) = \pm 0.05$ TPa^{-1} , $u(\kappa_{s,m}) = \pm 0.05 \times 10^{-15}$ $\text{m}^3 \cdot \text{Pa}^{-1} \cdot \text{mol}^{-1}$, $u(L_f) = \pm 0.01 \times 10^{-11}$ m, $u(p) = \pm 0.002$ MPa

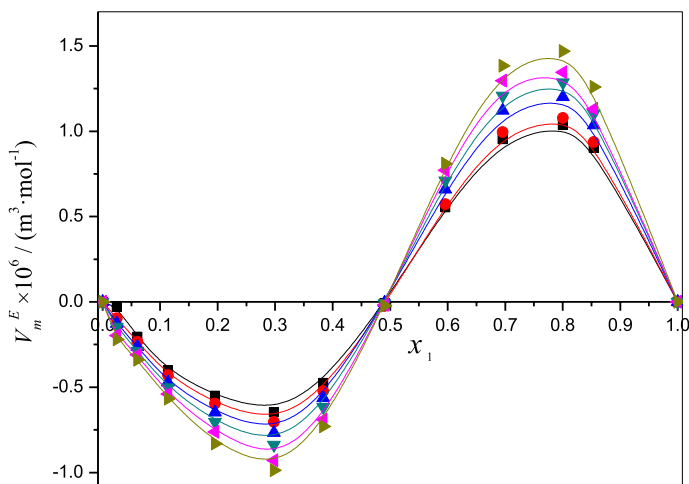


Fig. 3 Excess molar volume V_m^E versus mole fraction of [Bmim][NTf₂] (x_1) in the binary mixture of [Bmim][NTf₂]+2-PR at 298.15 K (filled square), 303.15 K (red filled circle), 308.15 K (blue filled triangle), 313.15 K (green filled inverted triangle), 318.15 K (pink filled left sided triangle) and 323.15 K (light green filled right sided triangle). The symbols represent experimental and the solid curves represent the values calculated from the Redlich–Kister equation (Eq. 11) (Color figure online)

the dissociated ionic liquid at higher temperature. Therefore, at higher temperatures the ion–dipole interactions between unlike species (ions from ionic liquid and dipoles of 2-PR species) become more significant due to availability of a greater number of alkanol dipoles, leading to contraction in volume, thus decreasing the volume of the mixture [18]. The reverse trend was observed in [Bmim][NTf₂] rich region, i.e. that V_m^E values become more positive as the temperature increased. This trend can be attributed to the dispersion of forces and non-specific interactions between the chemical species.

Isentropic compressibility (κ_s) was calculated from the Newton–Laplace equation as,

$$\kappa_s = \frac{1}{u^2 \rho} \quad (4)$$

Molar isentropic compressibility ($\kappa_{s,m}$) is given by the equation,

$$\kappa_{s,m} = V_m \kappa_s \quad (5)$$

The non-linear variation of isentropic compressibility as a function of composition of liquid mixture is sufficient evidence for the existence of molecular interactions in solutions [25]. In this work, a non-linear variation of κ_s was observed with the mole fraction of [Bmim][NTf₂] in the liquid mixture with the values of κ_s increasing with increasing temperature (Fig. 4). This phenomenon of κ_s indicates the formation of a complex in the liquid mixture. The increasing values of $\kappa_{s,m}$ (Table 4), with the mole fraction of [Bmim][NTf₂] and temperature, show that the intermolecular interactions are leading to the formation of a complex in the mixture.

Excess isentropic compressibility (κ_s^E) was calculated from the following relation [26–29],

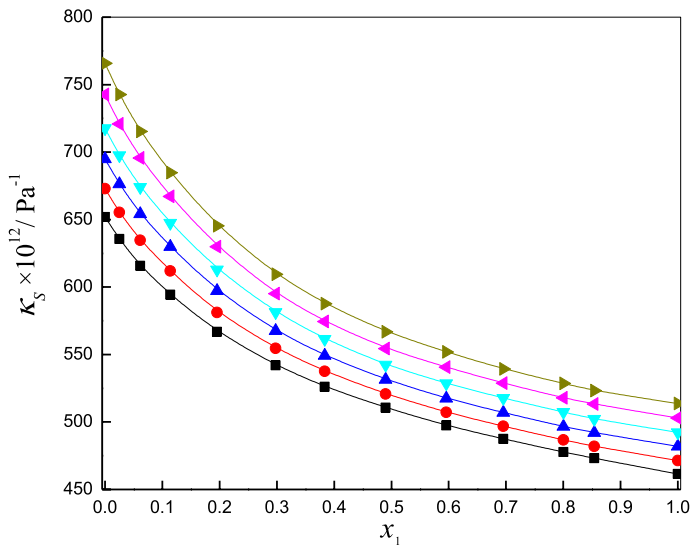


Fig. 4 Isentropic compressibility κ_s versus mole fraction of [Bmim][NTf₂] (x_1) in the binary mixture of [Bmim][NTf₂] + 2-PR at 298.15 K (filled square), 303.15 K (red filled circle), 308.15 K (blue filled triangle), 313.15 K (green filled inverted triangle), 318.15 K (pink filled left sided triangle) and 323.15 K (light green filled right sided triangle) (Color figure online)

$$\kappa_s^E = \kappa_s - \kappa_s^{\text{id}} = \kappa_s - \sum_{i=1}^2 \phi_i \left[\kappa_{s,i} + \frac{TV_i(\alpha_i^2)}{C_{p,i}} \right] - \left\{ \frac{T \left(\sum_{i=1}^2 x_i V_i \right) \left(\sum_{i=1}^2 \phi_i \alpha_i \right)^2}{\sum_{i=1}^2 x_i C_{p,i}} \right\} \quad (6)$$

where ϕ_i , $\kappa_{s,i}$, V_i , α_i , $C_{p,i}$, and x_i represent the volume fraction, isentropic compressibility, molar volume, coefficient of isobaric thermal expansion, heat capacity and mole fraction of pure components, respectively. From the density values, the isobaric coefficient of thermal expansion was calculated from the following equation,

$$\alpha = -\frac{1}{\rho} \left(\frac{\partial \rho}{\partial T} \right)_p \quad (7)$$

The variation of κ_s^E with volume fraction of [Bmim][NTf₂] (ϕ_1) in the binary mixture is shown in Fig. 5. It was observed that at all studied temperatures κ_s^E values of [Bmim][NTf₂] + 2-PR are negative over the complete composition range. The negative κ_s^E values indicate the strong attractive interactions due to the solvation of ions in the mixture. Further, these negative values indicate that the solvent species around the solute are less compressible than the solvent species in the bulk solutions. Increasing the concentration of IL decreases the negative values of κ_s^E at all temperatures. This might be due to the decrease in attraction of 2-PR and [Bmim][NTf₂] species in the [Bmim][NTf₂] rich concentration

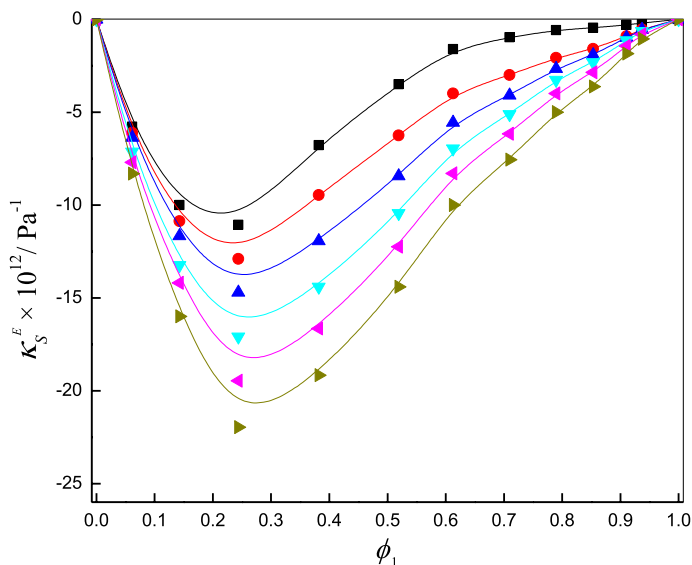


Fig. 5 Excess isentropic compressibility κ_s^E versus volume fraction of [Bmim][NTf₂] (ϕ_1) in the binary mixture of [Bmim][NTf₂] + 2-PR at 298.15 K (filled square), 303.15 K (red filled circle), 308.15 K (blue filled triangle), 313.15 K (green filled inverted triangle), 318.15 K (pink filled left sided triangle) and 323.15 K (light green filled right sided triangle). The symbols represent experimental and the solid curves represent the values calculated from Redlich–Kister equation (Eq. 11) (Color figure online)

region. These discrepancies may vary from IL to IL, solvent to solvent and also depend on the nature as well as structural arrangement of IL and solvent.

To understand the nature of intermolecular interactions, Jacobson suggested an empirical relation for calculating the intermolecular free length (L_f) [30],

$$L_f = K_j \sqrt{\kappa_s} \quad (8)$$

where K_j is the Jacobson's constant, which depends on temperature. Its value is $(93.875 + 0.375T) \times 10^{-8}$.

The intermolecular free length values of [Bmim][NTf₂] + 2-PR, investigated at various temperatures, are shown in Table 4. It is observed that, in the studied temperature range, the L_f values of 2-PR are greater than the L_f values of [Bmim][NTf₂]. But, as the mole fraction of [Bmim][NTf₂] is increasing in the mixture the intermolecular free length values are decreasing. This behavior shows the presence of molecular interactions between the compounds of the liquid mixture. Further, as the temperature increases the L_f values increase. This increase in the intermolecular free length increases the distance between the surfaces of the two species, which in turn leads to the decrease in the speed of sound.

Excess intermolecular free length (L_f^E) was calculated from the following equation [31],

$$L_f^E = L_f - K_j \sqrt{\kappa_s^{\text{id}}} \quad (9)$$

The variations of L_f^E can be attributed to various types of molecular interactions. The physical effects like dispersion forces or weak dipole–dipole interactions give positive L_f^E values and the chemical effects, like the formation of charge transfer complexes or other complex forming interactions, including strong dipole–dipole interactions between component species,

give negative L_f^E values [7]. In this work, the negative values of L_f^E (Fig. 6) designate specific interactions between different species in the binary mixture. The large negative values of L_f^E indicate structural readjustments in the mixture, which may result in a less compressible liquid phase and closer packing.

Excess speed of sound (u^E) was estimated from the following equation [32],

$$u^E = u - u^{\text{id}} = u - (\rho^{\text{id}} \kappa_s^{\text{id}})^{-1/2} \quad (10)$$

where $\rho^{\text{id}} = \sum_{i=1}^2 \phi_i \rho_i$

Figure 7 shows the variations of excess speed of sound with mole fraction and temperature. The sign and magnitude of u^E plays an important role in describing the molecular rearrangements occurring as a result of specific interactions in the liquid mixture. Generally, the positive values of u^E indicate the presence of strong interactions and the negative values of u^E indicate the presence of weak interactions between unlike species in the mixture [33]. In the present work, positive u^E values were observed for the entire composition range at all the studied temperatures, indicating the presence of strong ion–dipole interactions between the components of the binary mixture.

All the excess values (V_m^E , κ_s^E , L_f^E and u^E) were fitted by the method of non-linear least squares to a Redlich–Kister polynomial equation of the type [34],

$$Y^E = x_1 x_2 \sum_{i=0}^n A_i (1 - 2x_1)^i \quad (11)$$

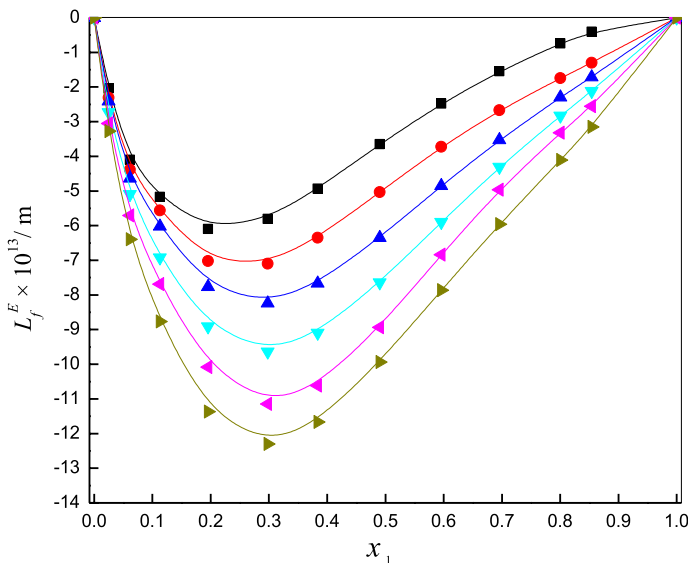


Fig. 6 Excess intermolecular free length L_f^E versus mole fraction of [Bmim][NTf₂] (x_1) in the binary mixture of [Bmim][NTf₂] + 2-PR at 298.15 K (filled square), 303.15 K (red filled circle), 308.15 K (blue filled triangle), 313.15 K (green filled inverted triangle), 318.15 K (pink filled left sided triangle) and 323.15 K (light green filled right sided triangle). The symbols represent experimental and the solid curves represent the values calculated from Redlich–Kister equation (Eq. 11) (Color figure online)

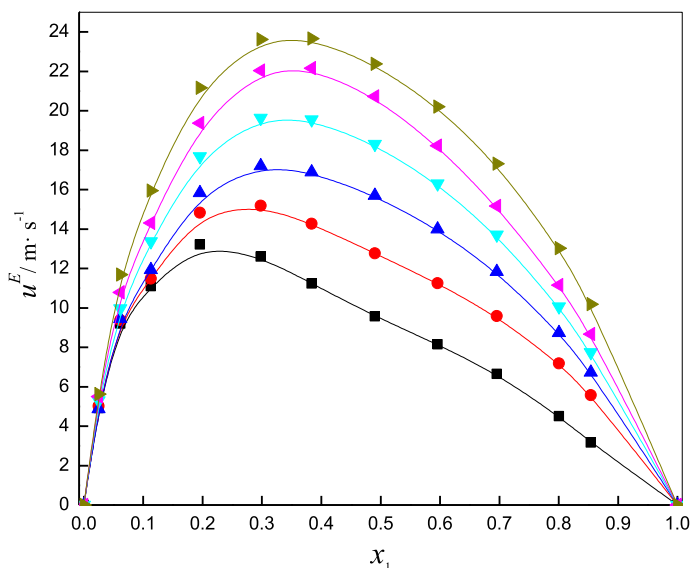


Fig. 7 Excess speed of sound u^E versus mole fraction of [Bmim][NTf₂] (x_1) in the binary mixture of [Bmim][NTf₂] + 2-PR at 298.15 K (filled square), 303.15 K (red filled circle), 308.15 K (blue filled triangle), 313.15 K (green filled inverted triangle), 318.15 K (pink filled left sided triangle) and 323.15 K (light green filled right sided triangle). The symbols represent experimental and the solid curves represent the values calculated from Redlich–Kister equation (Eq. 11) (Color figure online)

where x_1 is the mole fraction of [Bmim][NTf₂] and x_2 is the mole fraction of 2-PR. A_0 , A_1 , A_2 and A_3 are adjustable binary coefficients. The coefficients A_i were estimated using multi-parametric regression analysis based on the least-squares method. The number n of A_i parameters was optimized using the F -test. In each case, the optimum number of coefficients A_i was determined from an examination of the variation of standard deviation (σ). The coefficients and standard deviations obtained from Redlich–Kister polynomial equation are provided in Table 5. The standard deviation values show satisfactory results for the experimental values.

The partial molar volumes, $\bar{V}_{m,1}^o$ of component 1 ([Bmim][NTf₂]) and $\bar{V}_{m,2}^o$ of component 2 (2-PR) in the mixture over the entire composition range were calculated using the following relations [35],

$$\bar{V}_{m,1}^o = V_m^E + V_{m,1}^* + x_2 \left(\frac{\partial V_m^E}{\partial x_1} \right)_{T,p} \quad (12)$$

$$\bar{V}_{m,2}^o = V_m^E + V_{m,2}^* - x_1 \left(\frac{\partial V_m^E}{\partial x_1} \right)_{T,p} \quad (13)$$

where $\bar{V}_{m,1}^*$ and $\bar{V}_{m,2}^*$ are the molar volumes of the pure components [Bmim][NTf₂] and 2-PR, respectively. The derivative $\left(\frac{\partial V_m^E}{\partial x_1} \right)$ in Eqs. 12 and 13 is obtained by differentiating Eq. 11, which gives the following equations for $\bar{V}_{m,1}^o$ and $\bar{V}_{m,2}^o$:

Table 5 Coefficients (A_0, A_1, A_2, A_3) of the Redlich–Kister equation (Eq. 11) and corresponding standard deviations (σ) for 1-butyl-3-methylimidazolium bis(trifluoromethanesulfonyl) amide + 2-propoxyethanol from $T=(298.15$ to $323.15)$ K

Functions	A_0	A_1	A_2	A_3	σ
$T=298.15$ K					
$V_m^E \times 10^6$ ($\text{m}^3 \cdot \text{mol}^{-1}$)	0.183	-10.569	3.636	6.381	0.0518
$\kappa_s^E \times 10^{12}$ (Pa^{-1})	-23.877	-54.221	-37.690	-	0.0170
$L_j^E \times 10^{13}$ (m)	-14.115	-23.518	-20.224	-12.208	0.0668
u^E ($\text{m} \cdot \text{s}^{-1}$)	37.726	27.923	49.356	48.226	0.1756
$T=303.15$ K					
$V_m^E \times 10^6$ ($\text{m}^3 \cdot \text{mol}^{-1}$)	0.1227	-11.298	3.541	6.680	0.0324
$\kappa_s^E \times 10^{12}$ (Pa^{-1})	-34.855	-51.299	-34.145	-	0.0942
$L_j^E \times 10^{13}$ (m)	-19.629	-25.564	-21.833	-5.224	0.0912
u^E ($\text{m} \cdot \text{s}^{-1}$)	50.206	28.526	51.384	32.112	0.2412
$T=308.15$ K					
$V_m^E \times 10^6$ ($\text{m}^3 \cdot \text{mol}^{-1}$)	0.218	-12.643	4.148	8.126	0.0514
$\kappa_s^E \times 10^{12}$ (Pa^{-1})	-44.704	-53.040	-25.160	-	0.0321
$L_j^E \times 10^{13}$ (m)	-24.650	-27.448	-17.721	-1.839	0.0621
u^E ($\text{m} \cdot \text{s}^{-1}$)	61.232	28.679	40.524	21.612	0.1532
$T=313.15$ K					
$V_m^E \times 10^6$ ($\text{m}^3 \cdot \text{mol}^{-1}$)	0.221	-13.612	4.384	9.034	0.0615
$\kappa_s^E \times 10^{12}$ (Pa^{-1})	-54.270	-58.940	-23.290	-	0.0182
$L_j^E \times 10^{13}$ (m)	-29.613	-31.452	-18.137	0.302	0.1421
u^E ($\text{m} \cdot \text{s}^{-1}$)	72.143	32.108	41.364	22.423	0.3138
$T=318.15$ K					
$V_m^E \times 10^6$ ($\text{m}^3 \cdot \text{mol}^{-1}$)	0.217	-15.071	4.914	10.123	0.0913
$\kappa_s^E \times 10^{12}$ (Pa^{-1})	-62.888	-65.019	-25.643	-	0.0722
$L_j^E \times 10^{13}$ (m)	-35.672	-37.134	-18.792	7.122	0.1316
u^E ($\text{m} \cdot \text{s}^{-1}$)	81.789	40.143	38.561	9.541	0.2296
$T=323.15$ K					
$V_m^E \times 10^6$ ($\text{m}^3 \cdot \text{mol}^{-1}$)	0.198	-15.621	4.912	10.152	0.1023
$\kappa_s^E \times 10^{12}$ (Pa^{-1})	-72.737	-69.765	-27.840	-	0.0675
$L_j^E \times 10^{13}$ (m)	-38.504	-38.024	-27.324	-0.172	0.0926
u^E ($\text{m} \cdot \text{s}^{-1}$)	88.561	33.128	51.763	22.712	0.2352

$$\bar{V}_{m,1}^0 = V_{m,1}^* + x_2^2 \sum_{i=0}^n A_i (1 - 2x_1)^i - 2x_1 x_2^2 \sum_{i=1}^n i A_i (1 - 2x_1)^{i-1} \quad (14)$$

$$\bar{V}_{m,2}^0 = V_{m,2}^* + x_1^2 \sum_{i=0}^n A_i (1 - 2x_1)^i + 2x_1^2 x_2 \sum_{i=1}^n i A_i (1 - 2x_1)^{i-1} \quad (15)$$

The excess partial molar volumes, $\bar{V}_{m,1}^{0E}$ and $\bar{V}_{m,2}^{0E}$, over the whole composition range were calculated by using the following relations,

$$\bar{V}_{m,1}^{\text{oE}} = \bar{V}_{m,1}^{\text{o}} - V_{m,1}^* \quad (16)$$

$$\bar{V}_{m,2}^{\text{oE}} = \bar{V}_{m,2}^{\text{o}} - V_{m,2}^* \quad (17)$$

Another important property describing the behavior of the solution is the partial molar volume of solution at infinite dilution. By setting $x_2 = 1$ in Eq. 14, we get the partial molar volume of [Bmim][NTf₂] at infinite dilution in 2-PR.

$$\bar{V}_{m,1}^{\text{o},\infty} = V_{m,1}^* + \sum_{i=0}^n A_i(1)^i \quad (18)$$

Similarly, by putting $x_2 = 0$ in Eq. 15, we get the partial molar volume of 2-PR at infinite dilution in [Bmim][NTf₂].

$$\bar{V}_{m,2}^{\text{o},\infty} = V_{m,2}^* + \sum_{i=0}^n A_i(-1)^i \quad (19)$$

The excess partial molar volumes, $\bar{V}_{m,1}^{\text{oE},\infty}$ of [Bmim][NTf₂] and $\bar{V}_{m,2}^{\text{oE},\infty}$ of 2-PR at infinite dilution were determined using

$$\bar{V}_{m,1}^{\text{oE},\infty} = \bar{V}_{m,1}^{\text{o},\infty} - V_{m,1}^* \quad (20)$$

$$\bar{V}_{m,2}^{\text{oE},\infty} = \bar{V}_{m,2}^{\text{o},\infty} - V_{m,2}^* \quad (21)$$

The values of $\bar{V}_{m,1}^{\text{o}}$ and $\bar{V}_{m,2}^{\text{o}}$ as functions of mole fraction of [Bmim][NTf₂] and temperature are given in Table 6. We can observe that the values of $\bar{V}_{m,1}^{\text{o}}$ and $\bar{V}_{m,2}^{\text{o}}$ in the mixture, are different from their respective individual values in the pure states. The lower values indicate the contraction of volume and the higher values indicate the expansion of volume, upon mixing of [Bmim][NTf₂] with 2-PR. The variations of $\bar{V}_{m,1}^{\text{o}}$ and $\bar{V}_{m,2}^{\text{o}}$ with mole fraction of [Bmim][NTf₂] and temperature are shown in Figs. 8 and 9 respectively. In general, the negative $\bar{V}_{m,1}^{\text{oE}}$ and $\bar{V}_{m,2}^{\text{oE}}$ values indicate the presence of significant solute–solvent interactions between unlike species and the positive $\bar{V}_{m,1}^{\text{oE}}$ and $\bar{V}_{m,2}^{\text{oE}}$ values indicate the presence of significant solute–solute or solvent–solvent interactions between like species in the mixture [36]. We can observe from Figs. 8 and 9 that the values of $\bar{V}_{m,1}^{\text{oE}}$ and $\bar{V}_{m,2}^{\text{oE}}$ are negative for the lower concentrations of [Bmim][NTf₂] and positive for the higher concentrations of [Bmim][NTf₂] in the mixture. The negative $\bar{V}_{m,1}^{\text{oE}}$ and $\bar{V}_{m,2}^{\text{oE}}$ values indicate that [Bmim][NTf₂]–2-PR interactions are stronger than [Bmim][NTf₂]–[Bmim][NTf₂] or 2-PR–2-PR interactions and the positive $\bar{V}_{m,1}^{\text{oE}}$ and $\bar{V}_{m,2}^{\text{oE}}$ values indicate that [Bmim][NTf₂]–2-PR interactions are weaker than [Bmim][NTf₂]–[Bmim][NTf₂] or 2-PR–2-PR interactions.

The values of $\bar{V}_{m,1}^*$, $\bar{V}_{m,1}^{\text{o},\infty}$, $\bar{V}_{m,1}^{\text{oE},\infty}$, $V_{m,2}^*$, $\bar{V}_{m,2}^{\text{o},\infty}$ and $\bar{V}_{m,2}^{\text{oE},\infty}$ for the pure compounds [Bmim][NTf₂] and 2-PR, at the investigated temperatures, are listed in Table 7. The negative

Table 6 Partial molar volumes of 1-butyl-3-methylimidazolium bis(trifluoromethanesulfonyl) amide ($\bar{V}_{m,1}^0$) and 2-propoxyethanol ($\bar{V}_{m,2}^0$) with mole fraction (x_1) of 1-butyl-3-methylimidazolium bis(trifluoromethanesulfonyl) amide in the binary mixture of 1-butyl-3-methylimidazolium bis(trifluoromethanesulfonyl) amide + 2-propoxyethanol from $T=(293.15$ to $323.15)$ K at pressure $p=0.1$ MPa

x_1	$\bar{V}_{m,1}^0 \times 10^6$ ($\text{m}^3 \cdot \text{mol}^{-1}$)	$\bar{V}_{m,2}^0 \times 10^6$ ($\text{m}^3 \cdot \text{mol}^{-1}$)
$T=298.15$ K		
0	291.34	114.80
0.0251	290.03	114.82
0.0614	288.88	114.87
0.1131	288.38	114.91
0.1957	289.34	114.72
0.2980	291.63	113.96
0.3837	293.35	113.08
0.4901	294.47	112.24
0.5958	294.39	112.38
0.6956	293.59	113.88
0.8003	292.59	116.88
0.8543	292.19	118.78
1	291.81	122.87
$T=303.15$ K		
0	292.31	115.36
0.0251	290.87	115.38
0.0614	289.59	115.43
0.1131	289.03	115.48
0.1957	290.04	115.28
0.2980	292.52	114.46
0.3837	294.37	113.51
0.4901	295.56	112.61
0.5958	295.47	112.77
0.6956	294.61	114.39
0.8003	293.55	117.57
0.8543	293.13	119.56
1	292.75	123.53
$T=308.15$ K		
0	293.61	115.92
0.0251	291.92	115.94
0.0614	290.40	116.01
0.1131	289.70	116.07
0.1957	290.79	115.85
0.2980	293.56	114.93
0.3837	295.63	113.86
0.4901	296.96	112.87
0.5958	296.83	113.08
0.6956	295.84	114.93
0.8003	294.65	118.50
0.8543	294.19	120.69
1	293.79	124.72
$T=313.15$ K		
0	294.62	116.49
0.0251	292.74	116.51

Table 6 (continued)

x_1	$\bar{V}_{m,1}^{\circ} \times 10^6 \text{ (m}^3 \cdot \text{mol}^{-1}\text{)}$	$\bar{V}_{m,2}^{\circ} \times 10^6 \text{ (m}^3 \cdot \text{mol}^{-1}\text{)}$
0.0614	291.06	116.58
0.1131	290.26	116.65
0.1957	291.44	116.41
0.2980	294.47	115.41
0.3837	296.73	114.25
0.4901	298.17	113.17
0.5958	298.01	113.42
0.6956	296.93	115.45
0.8003	295.64	119.33
0.8543	295.15	121.66
1	294.74	125.64
$T=318.15 \text{ K}$		
0	296.46	117.06
0.0251	294.09	117.09
0.0614	291.91	117.18
0.1131	290.78	117.28
0.1957	291.97	117.04
0.2980	295.38	115.90
0.3837	297.95	114.58
0.4901	299.56	113.38
0.5958	299.31	113.74
0.6956	298.05	116.11
0.8003	296.62	120.39
0.8543	296.11	122.79
1	295.77	125.41
$T=323.15 \text{ K}$		
0	296.42	117.64
0.0251	294.25	117.66
0.0614	292.31	117.75
0.1131	291.42	117.82
0.1957	292.82	117.54
0.2980	296.35	116.37
0.3837	298.98	115.02
0.4901	300.64	113.77
0.5958	300.45	114.08
0.6956	299.18	116.45
0.8003	297.69	120.92
0.8543	297.13	123.59
1	296.67	127.94

Standard uncertainties u are $u(T) = \pm 0.01 \text{ K}$, $u(x_1) = \pm 1 \times 10^{-4}$, $u(\bar{V}_{m,1}^{\circ}) = \pm 0.05 \times 10^{-6} \text{ m}^3 \cdot \text{mol}^{-1}$, $u(\bar{V}_{m,2}^{\circ}) = \pm 0.05 \times 10^{-6} \text{ m}^3 \cdot \text{mol}^{-1}$, $u(p) = \pm 0.002 \text{ MPa}$

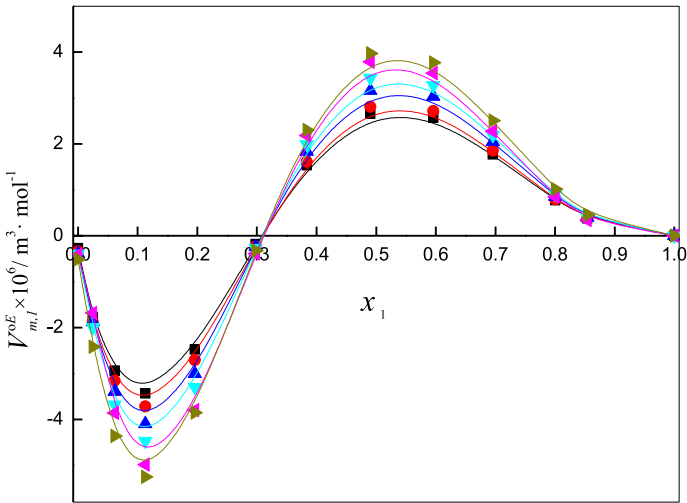


Fig. 8 Excess partial molar volume $\bar{V}_{m,1}^{OE}$ of [Bmim][NTf₂] versus mole fraction of [Bmim][NTf₂] (x_1) in the binary mixture of [Bmim][NTf₂] + 2-PR at 298.15 K (filled square), 303.15 K (red filled circle), 308.15 K (blue filled triangle), 313.15 K (green filled inverted triangle), 318.15 K (pink filled left sided triangle) and 323.15 K (light green filled right sided triangle) (Color figure online)

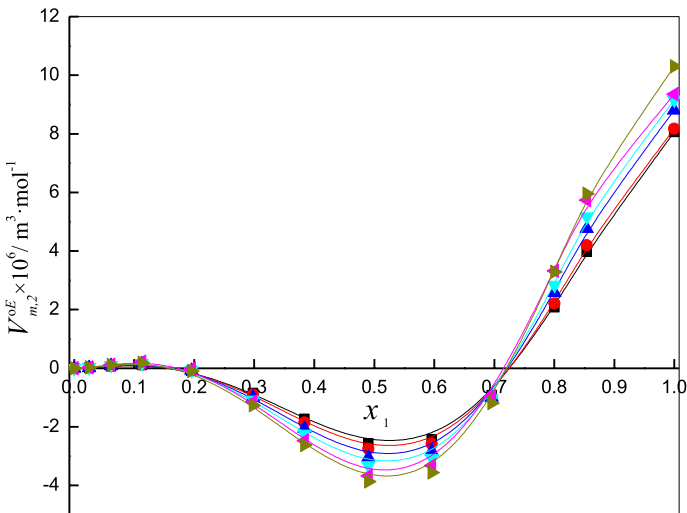


Fig. 9 Excess partial molar volume $\bar{V}_{m,2}^{OE}$ of 2-PR versus mole fraction of [Bmim][NTf₂] (x_1) in the binary mixture of [Bmim][NTf₂] + 2-PR at 298.15 K (filled square), 303.15 K (red filled circle), 308.15 K (blue filled triangle), 313.15 K (green filled inverted triangle), 318.15 K (pink filled left sided triangle) and 323.15 K (light green filled right sided triangle) (Color figure online)

values of $\bar{V}_{m,1}^{OE,\infty}$ indicate that the molar volume of [Bmim][NTf₂] in the mixture is smaller than its molar volume in the pure state, i.e., there is a contraction in the volume on mixing [Bmim][NTf₂] with 2-PR. The increase in the negative values of $\bar{V}_{m,1}^{OE,\infty}$ with the increase in temperature is attributed to the expansion in volume of the mixture, which allows more

Table 7 Molar volumes of 1-butyl-3-methylimidazolium bis(trifluoromethanesulfonyl) amide ($V_{m,1}^*$), 2-propoxyethanol ($V_{m,2}^*$), partial molar volumes at infinite dilution for 1-butyl-3-methylimidazolium bis(trifluoromethanesulfonyl) amide ($\bar{V}_{m,1}^{0,\infty}$), 2-propoxyethanol ($\bar{V}_{m,2}^{0,\infty}$) and excess partial molar volumes at infinite dilution for 1-butyl-3-methylimidazolium bis(trifluoromethanesulfonyl) amide ($\bar{V}_{m,1}^{oE,\infty}$), 2-propoxyethanol ($\bar{V}_{m,2}^{oE,\infty}$) from $T=(293.15$ to $323.15)$ K at pressure $p=0.1$ MPa

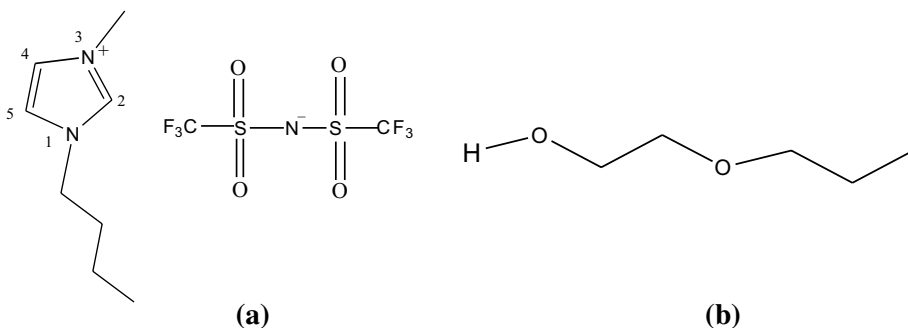
T/K	$V_{m,1}^* \times 10^6$ ($\text{m}^3 \cdot \text{mol}^{-1}$)	$\bar{V}_{m,1}^{0,\infty} \times 10^6$ ($\text{m}^3 \cdot \text{mol}^{-1}$)	$\bar{V}_{m,1}^{oE,\infty} \times 10^6$ ($\text{m}^3 \cdot \text{mol}^{-1}$)	$V_{m,2}^* \times 10^6$ ($\text{m}^3 \cdot \text{mol}^{-1}$)	$\bar{V}_{m,2}^{0,\infty} \times 10^6$ ($\text{m}^3 \cdot \text{mol}^{-1}$)	$\bar{V}_{m,2}^{oE,\infty} \times 10^6$ ($\text{m}^3 \cdot \text{mol}^{-1}$)
298.15	291.81	291.34	-0.47	114.80	122.87	8.06
303.15	292.75	292.27	-0.48	115.36	123.53	8.17
308.15	293.79	293.26	-0.53	115.92	124.72	8.80
313.15	294.74	294.17	-0.56	116.49	125.64	9.16
318.15	295.77	295.07	-0.69	117.06	126.41	9.35
323.15	296.67	295.92	-0.75	117.64	127.94	10.30

Standard uncertainties u are $u(T)=\pm 0.01$ K, $u(x_1)=\pm 1 \times 10^{-4}$, $u(V_{m,1}^*, V_{m,2}^*)=\pm 0.05 \times 10^{-6}$ $\text{m}^3 \cdot \text{mol}^{-1}$, $u(\bar{V}_{m,1}^{0,\infty}, \bar{V}_{m,2}^{0,\infty})=\pm 0.05 \times 10^{-6}$ $\text{m}^3 \cdot \text{mol}^{-1}$, $u(\bar{V}_{m,1}^{oE,\infty}, \bar{V}_{m,2}^{oE,\infty})=\pm 0.05 \times 10^{-6}$ $\text{m}^3 \cdot \text{mol}^{-1}$, $u(p)=\pm 0.002$ MPa

favorable fitting of smaller 2-PR species into the voids created by larger [Bmim][NTf₂] species at higher temperature.

The imidazolium salts contain a delocalized 3-center-4-electron configuration across the N₁-C₂-N₃ moiety, a double bond between C₄ and C₅ at the opposite side of the ring and a weak delocalization in the central region [37]. The hydrogen atoms C₂-H, C₄-H and C₅-H carry almost the same charge, but the carbon C₂ is positively charged owing to the electron deficit in the C=N bond, whereas C₄ and C₅ are practically neutral. The resulting acidity of the hydrogen atoms is the key to understand the properties of these ionic liquids (Scheme 1).

FT-IR spectra of pure 2-PR, pure [Bmim][NTf₂] and also for different mole fractions of [Bmim][NTf₂] ($x_1=0.2980$, 0.4901 and 0.8003) in the binary mixture were recorded from 500 to 3500 cm^{-1} (Fig. 10). In order to study the effects of molecular interactions on the [Bmim] cation, the CH stretching region between 2800 and 3200 cm^{-1} was analyzed. The signals between 2800 and 3000 cm^{-1} result from aliphatic CH groups in the butyl moiety [38–42]. The signals between 3000 and 3200 cm^{-1} can be assigned to CH modes originating from the aromatic imidazolium ring and also from C₂-H to C_{4,5}-H stretching vibrations [41]. The addition of 2-PR to the ionic liquid leads to a blue shift in imidazolium C-H



Scheme 1 Schematic structures for **a** [Bmim][NTf₂] and **b** 2PE

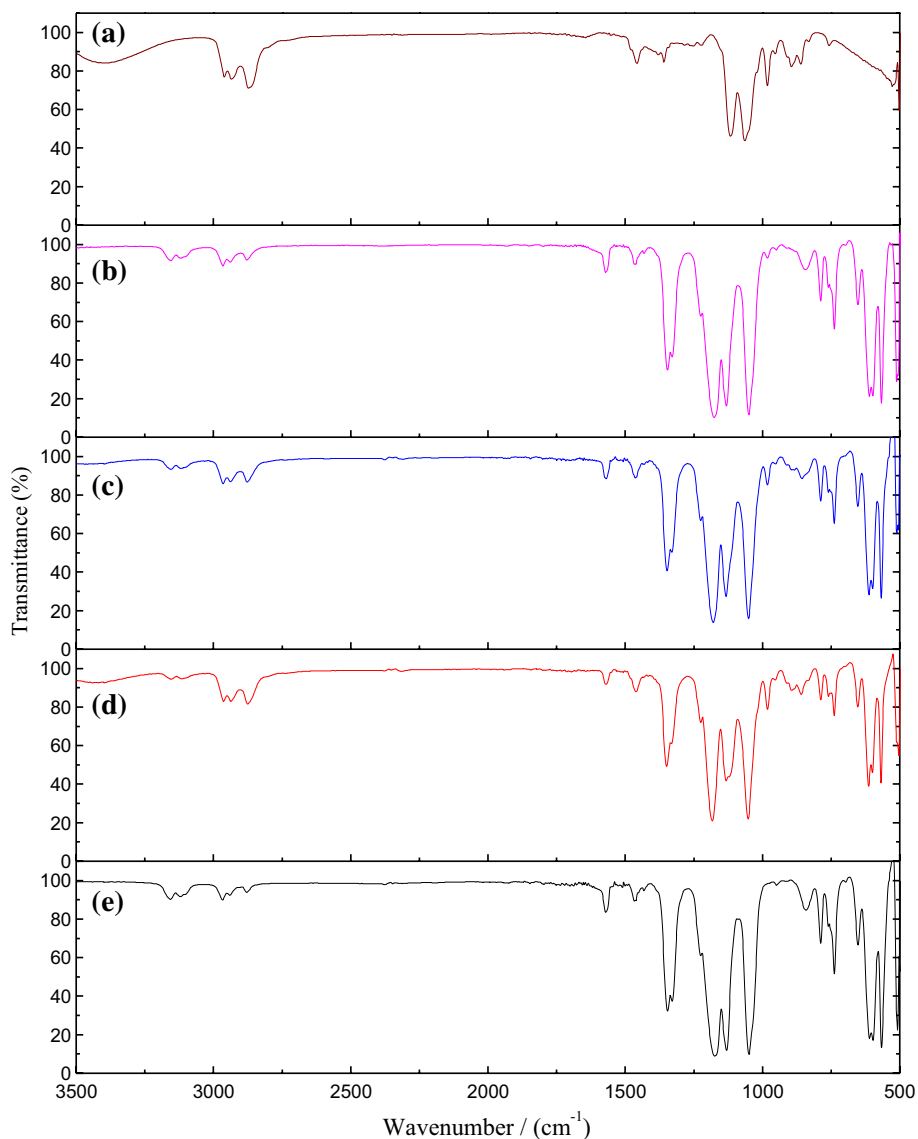


Fig. 10 FT-IR spectra of **a** pure 2-PR, **b** $x_1=0.2980$, **c** $x_1=0.4901$, **d** $x_1=0.8003$ and **e** pure [Bmim][NTf₂]

stretching vibrations. Similar molecular interactions were observed in the binary mixtures of imidazolium ionic liquids with other molecular solvents [6, 43–45]. In the case of the [NTf₂] anion, FT-IR spectra in the range from 630 to 680 cm⁻¹ were analyzed. The peak at 653 cm⁻¹ in the pure [Bmim][NTf₂] can be assigned to the S–N–S bending mode. The transmittance decreased with increasing mole fractions of [Bmim][NTf₂], indicating the presence of interactions between [NTf₂] anions and dipoles of 2PE.

The interaction mechanism of 2PE molecules with the cation and anion is different in nature. The C–H groups in the [Bmim] cation and nitrogen in [NTf₂] anion are characteristic groups interacting with 2-PR molecules. By studying the ATR-FTIR, we can predict that the addition

of [Bmim][NTf₂] to 2-PR influenced (i) C–H vibrations of [Bmim]⁺ cation; (ii) S–N–S bending mode of [NTf₂] anion; (iii) O–H stretching of 2-PR. Thus the FT-IR spectroscopy study indicates ion–dipole interactions in the binary mixture of [Bmim][NTf₂] and 2-PR.

4 Conclusions

Densities and speeds of sound were measured for the pure and binary mixture of [Bmim][NTf₂]+2-PR for various mole fractions at temperatures from $T=(298.15$ to $323.15)$ K under atmospheric pressure. From these experimental values, various acoustical and thermodynamic parameters were calculated. The intermolecular interactions between the binary mixture of [Bmim][NTf₂] and 2-PR were analyzed by studying the variations in the parameters determined. The negative excess molar volume indicate that more efficient packing are taking place when [Bmim][NTf₂] was added with 2-PR. The negative values of excess intermolecular free length designated the structural readjustments in the mixture leading to a less compressible liquid phase and closer packing of species. The positive excess speed of sound values designated the presence of strong ion–dipole interactions between the components of the binary mixture. Satisfactory correlations for the excess parameters were obtained by fitting them with the Redlich–Kister polynomial equation. The FT-IR spectra analysis indicated the formation of hydrogen bonding between [Bmim][NTf₂] and 2-PR.

Acknowledgements The authors would like to acknowledge the financial support of the DST-SERB, Research Project No. ECR/2016/000517 dated 24 November 2016, New Delhi, and are thankful to the Management of Vasireddy Venkatadri Institute of Technology, Nambur, Andhra Pradesh for the encouragement towards their research. One of the authors (G. Prasad) is thankful to the Management, Principal and HOD – AS&H, SASI Institute of Technology & Engineering, Tadepalligudem, Andhra Pradesh for their encouragement towards research.

References

1. Rogers, R.D., Seddon, K.R.: *Ionic Liquids—Industrial Applications to Green Chemistry*. ACS Symposium Series 818, Washington, DC, American Chemical Society, (2002)
2. Plechkova, N.V., Seddon, K.R.: Applications of ionic liquids in the chemical industry. *Chem. Soc. Rev.* **37**, 123–150 (2008)
3. Chiappe, C., Pieraccini, D.: Ionic liquids: solvent properties and organic reactivity. *J. Phys. Org. Chem.* **18**, 275–297 (2005)
4. Huddleston, J.G., Visser, A.E., Reichert, W.M., Willauer, H.D., Broker, G.A., Rogers, R.D.: Characterization and comparison of hydrophilic and hydrophobic room temperature ionic liquids incorporating the imidazolium cation. *Green Chem.* **3**, 156–164 (2001)
5. Rao, S.G., Mohan, T.M., Krishna, T.V., Krishna, T.S., Rao, B.S.: Density, refractive index and speed of sound of the binary mixture of 1-butyl-3-methylimidazolium tetrafluoroborate + *N*-vinyl-2-pyrrolidinone from $T=(298.15$ to $323.15)$ K at atmospheric pressure. *J. Chem. Eng. Data* **60**, 886–894 (2015)
6. Rao, S.G., Mohan, T.M., Krishna, T.V., Narendra, K., Rao, B.S.: Thermophysical properties of 1-butyl-3 methylimidazolium tetrafluoroborate and *N*-methyl-2-pyrrolidinone as a function of temperature. *J. Mol. Liq.* **211**, 1009–1017 (2015)
7. Rao, V.S., Krishna, T.V., Mohan, T.M., Rao, P.M.: Partial molar volumes and partial molar isentropic compressibilities of 1-butyl-3-methylimidazolium tetrafluoroborate + *N*-methylaniline binary mixture at temperatures $T=(293.15$ to $323.15)$ K and atmospheric pressure. *J. Mol. Liq.* **220**, 813–822 (2016)
8. Rao, V.S., Krishna, T.V., Mohan, T.M., Rao, P.M.: Physicochemical properties of green solvent 1-ethyl-3-methylimidazolium tetrafluoroborate with aniline from $T=(293.15$ to $323.15)$ K at atmospheric pressure. *J. Chem. Thermodyn.* **104**, 150–161 (2017)

9. Dominguez, I., Gonzalez, E.J., Palomar, J., Dominguez, A.: Phase behavior of ternary mixtures {aliphatic hydrocarbon + aromatic hydrocarbon + ionic liquid}: experimental LLE data and their modeling by COSMO-RS. *J. Chem. Thermodyn.* **77**, 222–229 (2014)
10. Wang, S., Liu, J., Yuan, L., Cui, Z., Peng, J., Li, J., Zhai, M., Liu, W.: Towards understanding the color change of 1-butyl-3-methylimidazolium bis(trifluoromethylsulfonyl)imide during gamma irradiation: an experimental and theoretical study. *Phys. Chem. Phys.* **16**, 18729–18735 (2014)
11. Rybczynska, M.G., Sitarek, M.: Acoustic and volumetric properties of binary mixtures of ionic liquid 1-butyl-3-methylimidazolium bis(trifluoromethylsulfonyl)imide with acetonitrile and tetrahydrofuran. *J. Chem. Eng. Data* **59**, 1213–1224 (2014)
12. Salgado, J., Regueira, T., Lugo, L., Vijande, J., Fernández, J., García, J.: Density and viscosity of three (2,2,2-trifluoroethanol + 1-butyl-3-methylimidazolium) ionic liquid binary systems. *J. Chem. Thermodyn.* **70**, 101–110 (2014)
13. de Castro, C.A.N., Langa, E., Morais, A.L., Lopes, M.L.M., Lourenco, M.J.V., Santos, F.J.V., Santos, M.S.C.S., Lopes, J.N.C., Veiga, H.I.M., Macatrão, M., Esperanca, J.M.S.S., Marques, C.S., Rebelo, L.P.N., Afonso, C.A.M.: Studies on the density, heat capacity, surface tension and infinite dilution diffusion with the ionic liquids [C4mim][NTf₂], [C4mim][dca], [C2mim][EtOSO₃] and [Aliquat][dca]. *Fluid Phase Equilib.* **294**, 157–179 (2010)
14. Krummen, M., Wasserscheid, P., Gmehling, J.: Measurement of activity coefficients at infinite dilution in ionic liquids using the dilutor technique. *J. Chem. Eng. Data* **47**, 1411–1417 (2002)
15. Salinas, R., Franco, J., Lladosa, E., Monton, J.B.: Density, speed of sound, viscosity, and excess properties of binary mixtures formed by ethanol and bis(trifluorosulfonyl)imide-based ionic liquids. *J. Chem. Eng. Data* **60**, 525–540 (2015)
16. de Azevedo, R.G., Esperanc, J.M.S.S., Szydowski, J., Visak, Z.P., Pires, P.F., Guedes, H.J.R., Rebelo, L.P.N.: Thermophysical and thermodynamic properties of ionic liquids over an extended pressure range: [bmim][NTf₂] and [hmim][NTf₂]. *J. Chem. Thermodyn.* **37**, 888–899 (2005)
17. Troncoso, J., Cerdeirín, C.A., Sanmamed, Y.A., Roman, L., Rebelo, L.P.N.: Thermodynamic properties of imidazolium-based ionic liquids: densities, heat capacities, and enthalpies of fusion of [bmim][PF₆] and [bmim][NTf₂]. *J. Chem. Eng. Data* **51**, 1856–1859 (2006)
18. Krishna, T.S., Raju, K.T.S.S., Gowrisankar, M., Nain, A.K., Munibhadrayya, B.: Volumetric, ultrasonic and spectroscopic studies of molecular interactions in binary mixtures of 1-butyl-3-methylimidazolium hexafluorophosphate with 2-propoxyethanol at temperatures from 298.15 to 323.15 K. *J. Mol. Liq.* **216**, 484–495 (2016)
19. Pal, A., Bhardwaj, R.K.: Excess molar volumes and viscosities for binary mixtures of 2-propoxyethanol and of 2-isopropoxyethanol with propylamine and dipropylamine at (298.15, 308.15, and 318.15) K. *J. Chem. Eng. Data* **46**, 933–938 (2001)
20. Cwilinska, A., Klimczaka, M., Kinar, W.J., Kinar, C.M.: Excess molar volumes and deviations of the relative permittivity of the binary mixtures of 2-propoxyethanol with diethylene, triethylene, and tetraethylene glycols at various temperatures. *J. Chem. Thermodyn.* **40**, 476–482 (2008)
21. Reddy, M.S., Raju, K.T.S.S., Rao, A.S., Sharmila, N., Babu, B.H.: Study of thermophysical properties of the binary mixtures of ionic liquid 1-ethyl-3-methylimidazolium ethylsulfate and 2-propoxyethanol from $T=(298.15$ to $328.15)$ K at atmospheric pressure. *J. Chem. Thermodyn.* **101**, 139–149 (2016)
22. Kavitha, T., Vasantha, T., Venkatesu, P., Devi, R.S.R., Hofman, T.: Thermophysical properties for the mixed solvents of N-methyl-2-pyrrolidone with some of the imidazolium-based ionic liquids. *J. Mol. Liq.* **198**, 11–20 (2014)
23. Prasad, G., Reddy, K.M., Padamasuvarna, R., Mohan, T.M., Krishna, T.V.: Density and speed of sound of the binary mixture of 1-butyl-3-methylimidazolium bis (trifluoromethylsulfonyl) imide + 2-methoxyethanol from $T=(298.15$ to $323.15)$ K at atmospheric pressure. *J. Chem. Eng. Data* **62**(11), 3903–3914 (2017)
24. Prasad, G., Reddy, K.M., Padamasuvarna, R., Mohan, T.M., Krishna, T.V., Kumar, V.R.: Thermophysical properties of 1-butyl-3-methylimidazolium bis(trifluoromethylsulfonyl) imide with 2-ethoxyethanol from $T=(298.15$ to $323.15)$ K at atmospheric pressure. *J. Mol. Liq.* **251**, 335–344 (2018)
25. Fort, R.J., Moore, W.H.: Adiabatic compressibilities of binary liquid mixtures. *Trans. Faraday Soc.* **61**, 2102–2111 (1965)
26. Kiyohara, O., Benson, G.C.: Ultrasonic speeds and isentropic compressibility of *n*-alkanol + *n*-heptane mixture at 298.15K. *J. Chem. Thermodyn.* **11**, 861–873 (1979)
27. Douheret, G., Salgado, C., Davis, M.I., Loya, J.: Ultrasonic speeds and isentropic functions of 2-(2-alkoxy ethoxy) ethanol + water at 298.15 K. *Thermochim. Acta* **207**, 313–328 (1992)
28. Douheret, G., Holczer, M.B., Peryrelier, R., Davis, M.I.: Speeds of sound and excess volumetric properties of mixtures of water with 2-propanol and with ethylene glycol monoisopropyl ether at 298.15 K. *J. Chem. Eng. Data* **39**, 868–872 (1994)

29. Douheret, G., Pal, A., Davis, M.I.: Ultrasonic speeds and isentropic functions of (2-alkoxyethanol+ water) at 298.15 K. *J. Chem. Thermodyn.* **22**, 99–108 (1990)
30. Sekhar, M.C., Mohan, T.M., Krishna, T.V., Venkatesulu, A., Kumar, K.S.: Density, refractive index, speed of sound and computational studies on intermolecular interactions in binary mixtures of 2-chloroaniline with butanols (1-butanol, 2-butanol) at $T=(303.15$ to $318.15)$ K. *J. Solution Chem.* **44**, 237–263 (2015)
31. Rao, S.G., Mohan, T.M., Krishna, T.V., Raju, K.T.S.S., Rao, B.S.: Excess thermodynamic properties of ionic liquid 1-butyl-3-methylimidazolium tetrafluoroborate and *N*-octyl-2- pyrrolidone from $T=(298.15$ to $323.15)$ K at atmospheric pressure. *J. Chem. Thermodyn.* **89**, 286–295 (2015)
32. Douheret, G., Davis, M., Reis, J.C.R., Blandamer, M.J.: Isentropic compressibilities—Experimental origin and the quest for their rigorous estimation in thermodynamically ideal liquid mixtures. *Chem. Phys. Chem.* **2**, 148–161 (2001)
33. Kawaizumi, F., Ohno, M., Miyahara, Y.: Ultrasonic and volumetric investigation of aqueous solutions of amides. *Bull. Chem. Soc. Jpn* **50**, 2229–2236 (1977)
34. Redlich, O., Kister, A.T.: Algebraic representation of thermodynamic properties and the classification of solutions. *J. Ind. Eng. Chem.* **40**, 345–348 (1948)
35. Wang, H., Liu, W., Huang, J.: Densities and volumetric properties of a (xylene + dimethyl sulfoxide) at temperature from (293.15 to 353.15) K. *J. Chem. Thermodyn.* **36**, 743–752 (2004)
36. Hawrylak, B., Gracie, K., Palepu, R.: Thermodynamic properties of binary mixtures of butanediols with water. *J. Solution Chem.* **27**, 17–31 (1998)
37. Hunt, P.A., Kirchner, B., Welton, T.: Characterizing the electronic structure of ionic liquids: an examination of the 1-butyl-3-methylimidazolium chloride ion pair. *Chem. Eur. J.* **12**, 6762–6775 (2006)
38. Lassegues, J.C., Grondin, J., Cavagnat, D., Johansson, P.: New interpretation of the CH stretching vibrations in imidazolium-based ionic liquids. *J. Phys. Chem. A* **113**, 6419–6421 (2009)
39. Lassegues, J.C., Grondin, J., Cavagnat, D., Johansson, P.: Reply to the comment on new interpretation of the CH stretching vibrations in imidazolium-based ionic liquids. *J. Phys. Chem. A* **114**, 687–688 (2009)
40. Grondin, J., Lassegues, J.C., Cavagnat, D., Buffeteau, T., Johansson, P., Holomb, R.: Revisited vibrational assignments of imidazolium-based ionic liquids. *J. Raman Spectrosc.* **42**, 733–743 (2011)
41. Dhumal, N.R., Kim, H.J., Kiefer, J.: Electronic structure and normal vibrations of the 1-ethyl-3-methylimidazolium ethyl sulfate ion pair. *J. Phys. Chem. A* **115**, 3551–3558 (2011)
42. Shimomura, T., Fujii, K., Takamuku, T.: Effects of the alkyl-chain length on the mixing state of imidazolium based ionic liquid–methanol solutions. *Phys. Chem. Chem. Phys.* **12**, 12316–12324 (2010)
43. Noack, K., Leipertz, A., Kiefer, J.: Molecular interactions and macroscopic effects in binary mixtures of an imidazolium ionic liquid with water, methanol, and ethanol. *J. Mol. Struct.* **1018**, 45–53 (2012)
44. He, H., Chen, H., Zheng, Y., Zhang, X., Yao, X., Yu, Z., Zhang, S.: The hydrogen-bonding interactions between 1-ethyl-3-methylimidazolium lactate ionic liquid and methanol. *Aust. J. Chem.* **66**, 50–59 (2013)
45. Kiefer, J., Molina, M.M., Noack, K.: The peculiar nature of molecular interactions between an imidazolium ionic liquid and acetone. *Chem. Phys. Chem.* **13**, 1213–1220 (2012)

Affiliations

G. Prasad^{1,5} · K. Muralidhar Reddy² · R. Padamasuvarna¹ · T. Madhu Mohan³ · T. Vijaya Krishna³ · S. Govardhana Rao⁴

¹ Department of Physics, JNTUA-College of Engineering, Ananthapuramu, Andhra Pradesh, India

² Department of EIE, R.G.M. College of Engineering & Technology, Nandyal, Andhra Pradesh, India

³ Department of Physics, Vasireddy Venkatadri Institute of Technology, Nambur, Andhra Pradesh, India

⁴ Department of Physics, St. Mary's Group of Institutions Guntur, Guntur, Andhra Pradesh, India

⁵ Department of Physics, SASI Institute of Technology & Engineering, Tadepalligudem, Andhra Pradesh, India